AJNR

Influence of Geometric and Hemodynamic Parameters on Aneurysm Visualization during Three-Dimensional Rotational Angiography: An in Vitro Study

Ulrike U. Ernemann, Eckart Grönewäller, Frank B. Duffner, Oezlem Guervit, Joerg Claassen and Martin D. Skalej

Influence of Geometric and Hemodynamic Parameters on Aneurysm Visualization during Three-Dimensional Rotational Angiography: An in Vitro Study

Ulrike U. Ernemann, Eckart Grönewäller, Frank B. Duffner, Oezlem Guervit, Joerg Claassen, and Martin D. Skalej

BACKGROUND AND PURPOSE: Aneurysm depiction with three-dimensional (3D) rotational angiography is influenced by investigator-defined parameters such as image acquisition and contrast agent injection and by the hemodynamic pattern in the parent artery and aneurysm. To assess the impact of the geometric configuration of parent artery and aneurysm on the 3D visualization of saccular aneurysms, we studied silicone aneurysm models under pulsatile-flow conditions.

METHODS: Rotational angiography was performed in three bifurcation and three lateral aneurysm models with ostia of different widths. Three acquisition modalities (5, 8, and 14 seconds in duration, acquisition rate of 10 frames per second) and two techniques for the injection of contrast material (continuous flow and injection with an initial bolus) were applied. 3D reconstructions were obtained with a volume-rendering technique.

RESULTS: Bifurcation aneurysms were visualized with high accuracy. Filling deficits distant to the inflow zone could be compensated for with the bolus-injection technique, and complete depiction of aneurysm shape was achieved in the 8-second rotation with 20 mL of contrast agent. In lateral aneurysms, the accuracy of 3D reconstructions depended on the width of the ostium. Although rotational studies in wide-necked lateral aneurysms yielded adequate reconstructions, 3D visualization of small-necked aneurysms was incomplete with the preferential depiction of the distal shell, which represents the inflow zone into the aneurysmal lumen.

CONCLUSION: Contrast agent injection with the initial-bolus technique improved the depiction of aneurysms, compared with the continuous-flow method. Reconstructions of rotational studies of narrow-necked lateral aneurysms yielded incomplete visualization of the aneurysm.

Over the last few years, three-dimensional (3D) rotational angiography (RA) has evolved as a major diagnostic tool in the angiographic assessment of aneurysms before surgical or endovascular treatment (1–4). The core of 3D RA is the computation of 3D voxels from 2-dimensional (2D) projection images (5). Therefore, the precision and accuracy of the 3D reconstruction depends on the realistic and constant representation of the object of interest on the projection images throughout the entire rotational cycle (6).

However, technical and physiologic limitations lead to the collection of images with variable contrast across a single rotational dataset (6). Possible distortions of the acquisition system due to equipment vibration must be considered, along with the dilution of contrast material during blood flow and the degradation of data due to pulsation and inhomogeneity of the surrounding tissues.

The most relevant factor among the physiologic parameters is the inhomogeneous and incomplete filling of the aneurysmal sac with contrast material; this process depends on the flow into the aneurysm. Studies of aneurysmal hemodynamics in humans and silicone models with a laser Doppler technique have shown that the intraaneurysmal flow pattern is mainly determined by the geometric relationship between the aneurysm and the parent artery (7, 8). Results of angiographic and duplex studies in canine aneurysm models, as well as computer modeling, have con-

firmed that the intra-aneurysmal circulation is predictable according to the geometry of the parent artery–aneurysm complex (9, 10). Whereas bifurcation aneurysms reveal a rapid intra-aneurysmal circulation without evidence of vortex formation, lateral aneurysms show a distinct flow pattern with inflow at the distal extent of the ostium and a central low-flow vortical recirculation zone.

These hemodynamic phenomena influence visualization of the aneurysm with conventional digital subtraction angiography (DSA) and, consequently, with 3D reconstructions. The correlation between aneurysm depiction with 3D RA and the true anatomy of these lesions has been described on the basis of clinical experience during surgical treatment (11). Another means of evaluating the accuracy of 3D RA is to assess the relevance of 3D measurements in choosing the first coil used during endovascular treatment (4).

To our knowledge, an experimental evaluation of the anatomic accuracy of 3D RA in aneurysm imaging has not been described.

The purpose of this study was to investigate the influence of the geometric parameters, particularly the width of the ostium in relation to the size of the aneurysmal sac, on the 3D RA visualization of bifurcation and lateral aneurysms in silicone models under pulsatile-flow conditions. We also analyzed the impact of the number of projection images acquired during RA and of different techniques for injecting the contrast agent on image quality and on the expression of geometric parameters in 3D reconstructions.

Methods

Aneurysms were attached to silicone models of a right anterior circulation (Elastrat, Geneva, Switzerland) with inflow through the internal carotid artery (ICA) and outflow through the posterior cerebral artery, the middle cerebral artery (MCA) with two branches, and a dominant anterior cerebral artery (12). We studied three bifurcation aneurysms and three lateral ones with ostia of different sizes (Fig 1). Models 1 and 2 represent bifurcation aneurysms with a medium-sized aneurysm arising at a 45° angle from an axis-symmetrical MCA bifurcation with a small (model 1) or large (model 2) neck (Table 1). In addition, model 2 had a small aneurysm with wide ostium originating at a 45° angle from the junction of AcoA and both A2 segments.

Lateral aneurysms were investigated in models 3–5. Models 3 and 4 had simple-lobed, giant lateral aneurysms of the supraclinoid ICA, with a small ostium in model 3 and large ostium in model 4. Model 5 had a lobulated, giant lateral aneurysm with a medium-sized ostium.

Each model was placed into a Plexiglas container filled with distilled water and connected to a circuit fed by a pump simulating pulsatile blood flow (Shelley; Ontario, Canada). Flow parameters in the ICA were a peak flow of 7.9 mL/s, a systole-to-diastole ratio of 37.5:62.5, a rate of 75 beats per minute, and a stroke volume of 485 mL (13, 14).

A 4F vertebral catheter was inserted into the cervical segment of the ICA for the injection of contrast material.

RA was performed by using the frontal plane of a biplanar C arm (Neurostar TOP; Siemens, Forchheim, Germany). The rotational study covered an angular range of 200° and consisted of a rotational mask followed by a second run during the injection of contrast material. The duration of the rotational run was selected
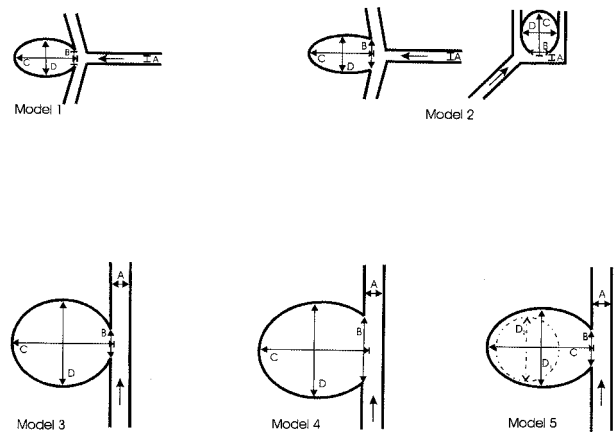

FIG 1. Aneurysm models 1–5. *Arrows* indicate the direction of blood flow. *A* indicates parent artery; *B*, ostium width, *C*, dome height; and *D*, dome diameter.

as 5, 8, or 14 seconds, corresponding to the acquisition of 50, 80, or 132 projection images. We investigated each model with these three modalities. Projection images were acquired with a 22-cm image intensifier by using a 1024-pixel matrix (3). Beam hardening was achieved by placing three 0.3-mm copper filters in front of the x-ray tube to compensate for the lack of bony structures surrounding the aneurysm models.

All models were investigated by using two protocols for the injection of contrast material: one for continuous flow and another divided into two phases with a bolus in the first and a lower flow rate in the second. This technique was derived from clinical experience that had shown that manual injection of an initial bolus resulted in earlier filling of the aneurysms on the projection images; consequently, this technique provided better visualization of the aneurysms on the 3D reconstructions. With the use of an angiographic injector (Angiomat Illumena; Liebel-Flarsheim, Medicor, Kerpen, Germany) 20 mL of a 300-mg/mL iodinated contrast material was administered for the 5- and 8-second runs, and 35 mL was used for the 14-second run (Table 2). In the bolus protocols, half of the contrast agent was injected as initial bolus, and half was used to maintain flow during the rest of the rotational sweep.

In the first part of the study, all models were investigated with the two protocols, and injections were timed to synchronize the arrival of contrast material at the ostium of the aneurysm with the start of image acquisition. In the second part, additional rotational studies with modified parameters were performed in the lateral aneurysm with the narrow neck. In the 8- and 14-second rotations with continuous flow, we increased the rate of the injection to 5 mL/s. For the 8-second rotation with the bolus technique, we injected an extra bolus at 5 mL/s over 2 seconds before starting image acquisition with the injection protocol for contrast agent bolus. In another experiment, the bolus velocity in the 8-second rotation was doubled.

Projection images were transferred to a workstation for 3D reconstruction (3D Virtuoso; Silicon Graphics). The first step in the reconstruction process is the computation of 2D axial images in a user-defined subvolume of the acquisition data. We used a 256-pixel matrix and a volume of interest (VOI) focused on the aneurysms and the adjacent main branches.

3D reconstructions of these images were visualized by using volume-rendering technique. The rendering parameters were chosen to achieve an anatomically correct representation of the parent arteries and main branches in the absence of background noise.

Two neuroradiologists (U.U.E., M.D.S.) who were blinded to the imaging parameters evaluated the 3D reconstructions by consensus opinion, according to the following criteria for overall image quality and visualization of the aneurysm: 1) homogeneous filling and anatomically correct visualization of the

TABLE 1: Dimensions in the models of bifucation and lateral aneurysm models

Model and Parent Artery*	Ostium Width, mm	Dome Height, mm	Dome Diameter, mm
1, MCA 3 × 3	4.5	16.5	10
2, MCA 3 × 3	8	16.5	10
AcoA 2 × 2	6	11	10
3, ICA 5 × 5.5	8	27	23
4, ICA 5 × 5.5	17	28	25.5 × 24
5, ICA 5 × 5.5	10.5	28	21
Second lobule	12	17	17

* AcoA indicates anterior communicating artery.

TABLE 2: Protocols used to inject the contrast material

Protocol	Duration of Rotational Run		
	5 Seconds	8 Seconds	14 Seconds
Continuous flow, mL/s	4.0	2.5	2.5
Initial bolus injection, mL/s			
First phase	5.0 over 2 s	5.0 over 2 s	4.0 over 4 s
Second phase	3.3 over 3 s	1.7 over 6 s	1.9 over 10 s

parent arteries and main branches, 2) plasticity of vessel structures and smoothness of the surfaces, 3) correct depiction of the shape of the aneurysm, 4) visualization of aneurysmal neck, and 5) measurement of diameter of the aneurysms on volume-rendered images in models in which complete visualization was achieved.

Results

Influence of Acquisition Parameters on 3D Reconstructions

In all model studies, the use of longer rotational runs with more projection images improved overall the image quality with regard to homogeneous filling of the parent arteries and main branches with contrast material and in terms of the plasticity of the vascular structures. The increased plasticity of vascular surfaces with additional projection images was particularly evident in the depiction of the neck of the aneurysm in relation to the parent artery (Fig 2).

Influence of the Injection Technique on 3D Reconstructions

In the 5- and 8-second rotational studies, the initial injection of the bolus of contrast agent yielded image quality better than that achieved with the continuous-flow technique (Fig 2B and C). The images were improved with regard to homogeneous filling of the vascular structures and plasticity. The 14-second rotations showed no substantial difference between the two injection techniques.

Influence of Geometric Parameters in Different Rotation and Injection Techniques

Bifurcation Aneurysms.—In both the 5- and 8-second rotations with continuous flow, model 1 (the small-necked aneurysm of the MCA bifurcation) showed an oval-shaped filling defect at the medial wall; this was distant to the inflow zone in the extension of the main axis of the MCA (Fig 3). This defect distorted the shape of the aneurysm, which simulated a concave outline of the wall. In the 8-second rotation with a bolus injection and in the 14-second rotations, this phenomenon was hardly perceptible.

The 8-second rotation with a bolus injection provided the most realistic 3D depiction of the aneurysm with use of 20 mL of contrast material. Measurements of the diameter of the aneurysms on volume-rendered 3D images obtained with that technique showed a mean difference of 0.1 mm compared with the known values. The 14-second rotations achieved higher plasticity and smoothness of vascular surfaces, but it provided no additional information about the geometry of the aneurysm.

The wide-neck aneurysm of the MCA bifurcation in model 2 revealed a filling defect smaller than the aneurysm with the tight neck. This circumscript defect at the lateral wall was clearly visible with the 5-second rotation with continuous flow, but it was only slightly visible with the 5-seconds rotation with a bolus injection and with the 8-second rotation with continuous flow. In the 8-second rotation with a bolus injection and in the 14-seconds rotations, the 3D image was in complete conformity with the model (Fig 2).

Diameter measurements obtained with the 8-second rotation and a bolus injection deviated from the known values by 0.1–0.2 mm.

The wide-neck aneurysm of the AcoA in model 2 showed the same filling pattern as that in the MCA aneurysm with large neck (Fig 2). A small filling defect at the wall opposite to the zone of inflow was prominent with the 5-second rotation and continuous flow. It was less conspicuous with the 5-second rotation with a bolus injection and with the 8-second rotation with continuous flow. No filling defect was seen with the 8-second rotation with a bolus injection and with the 14-second rotations.

3D measurements obtained in reconstructions of the 8-second rotation with a bolus injection showed a mean difference of 0.1–0.2 mm compared with the true diameters.

Lateral Aneurysms.—In the small-necked giant lateral aneurysm in model 3, only the distal aneurysmal shell could be distinctly visualized on the 3D reconstructions (Fig 4B). With more projection images, the homogeneity and plasticity of the images of the distal wall gradually increased, but complete depiction of the aneurysmal shape was not achieved. The level of contrast material along the proximal wall of the aneurysm was so low that this part of the 3D image could not be properly separated from the background noise.

In additional rotational studies performed with modified parameters, increased amounts of contrast agent (4–5 mL/s in the 8- and 14-second runs with continuous injection) did not notably alter the filling of the aneurysmal cavity. Contrast in the proximal wall was still insufficient (Fig 4C).
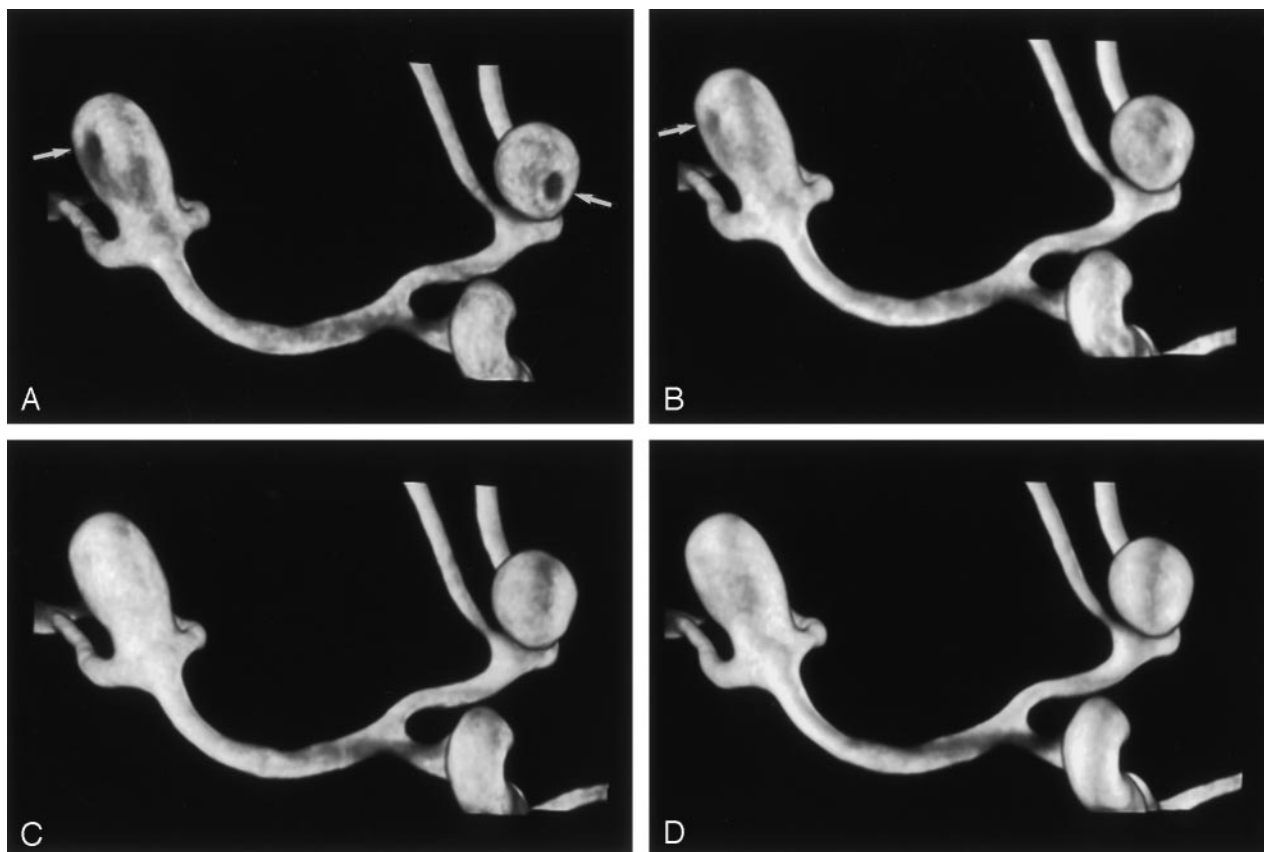
FIG 2.   Model 2, wide-necked aneurysm in the MCA bifurcation and AcoA. Voxel size, 0.25 mm.
   A, The 5-second rotation with continuous flow shows filling defects in both aneurysms (*arrows*).
   B, The 8-second rotation with continuous flow shows a slight defect in the MCA aneurysm (*arrow*).
   C, Accurate visualization of the aneurysm is achieved in the 8-second rotation with the bolus injection.
   D, The 14-second rotation with continuous flow has higher plasticity, but it does not provide any additional information about the geometry of the aneurysm.

FIG 3.   Model 1, small-necked aneurysm in the MCA bifurcation. Voxel size, 0.13 mm.
   A, The 8-second rotation with continuous flow shows a filling defect at the medial wall of the aneurysm (*arrow*).
   B, The 8-second rotation with bolus injection provides accurate 3D visualization of the shape of the aneurysm.
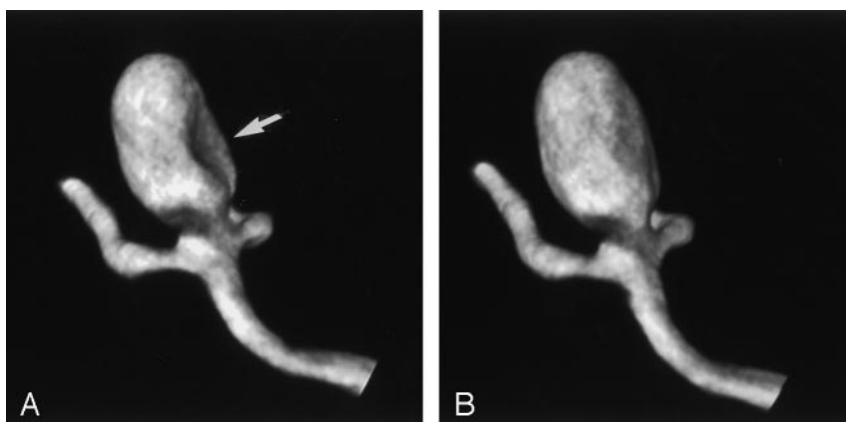
Slightly improved visualization with more solid filling of the distal third of the aneurysm was achieved by injecting an extra bolus of 10 mL (5 mL/s over 2 seconds) before the start of image acquisition in the 8-second run with the bolus technique.

Doubling the velocity of the initial bolus in the 8-second rotation caused a deterioration in image quality, resulting in a blurred appearance.

The shape of the giant lateral aneurysm with a large neck was adequately depicted in all rotational studies (Fig 5). The 5-second rotation showed small inhomogeneities in the wall; these were more prominent with the continuous-injection technique than with the bolus technique. The 8- and 14-seconds rotations enabled complete visualization of the aneurysm, with higher plasticity in the 14-second studies.

3D measurements of the diameters of the aneurysms in the 8-second rotation deviated from the known values by 0.2–0.3 mm.

In all rotational studies of the medium-necked, lobulated, giant lateral aneurysm in model 5, filling of the
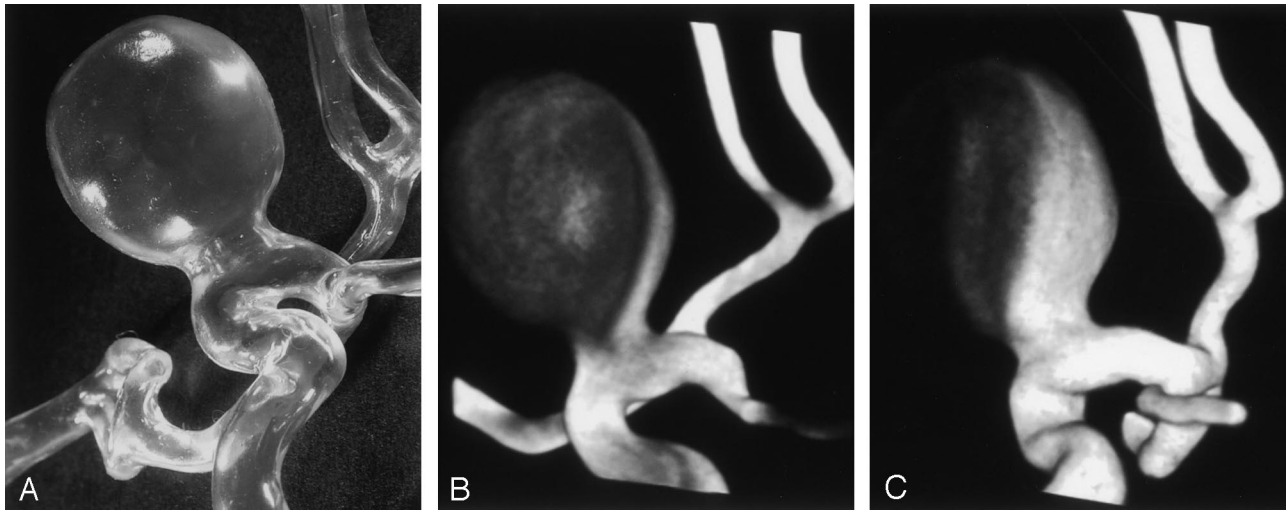
Fɪɢ 4.   Model 3, small-necked giant lateral aneurysm. Voxel size, 0.16 mm.
   A, The true shape of the aneurysm was not visualized on the 3D reconstruction.
   B, The 14-second rotation with a bolus injection reveals only the distal aneurysmal shell.
   C, In the 14-second rotation, the proximal wall of the aneurysm is not clearly delineated, even after the administration of contrast material at a rate of 5 mL/s.
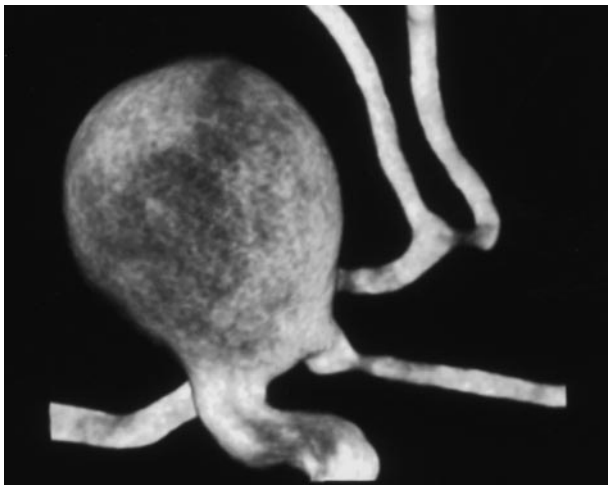

Fɪɢ 5.   Model 4, large-necked giant lateral aneurysm with large neck. Voxel size, 0.18 mm. The 8-second rotation with a bolus injection enables complete visualization of the shape of the aneurysm.

large sac was limited to the distal shell. With additional projection images, wall thickness and plasticity increased. Filling of the second lobule was more homogeneous. A bridge of contrast material could be visualized from the distal wall of the large sac to the proximal wall of the small lobule. In all studies, the level of filling in the small lobule was limited to the respective level in the large sac. Complete visualization of the shape of the aneurysm could not be achieved.

Discussion

The use of a silicone model of the cerebral arteries allowed us to consider the effects of pulsatile flow on the hemodynamics. Doppler measurements of flow velocities in lateral aneurysm models have shown that intra-aneurysmal flow is related to the pulsatility of perfusion with flow velocities in the center of the fundus, with 8–13% of the flow velocity in the parent artery under pulsatile perfusion and with 0.4% and 2% under nonpulsatile perfusion (8).

Limitations of our model were that the precise elasticity of the human vessel wall could not be reproduced and that the water surrounding the aneurysms has properties different from those of brain tissue. The effects the elements surrounding an aneurysm must be considered when the postprocessed images are evaluated because the background noise due to venous filling and the superposition of small arteries is higher in vivo than in the model.

As for the investigator-defined parameters in 3D RA, the different techniques of image acquisition and the injection of contrast material had considerable influence on the visualization of vessels.

Image acquisition is defined by the duration of the rotational run and by the number of projection images. With our machine (Neurostar TOP; Siemens) rotational studies were acquired at a fixed frame rate of 10 frames per second, which automatically linked the two parameters.

Longer rotational runs improve image quality by allowing more time for filling of the aneurysm with contrast material. This effect particularly applies to aneurysms with the hemodynamic pattern of the lateral aneurysm with a narrow neck. Although the injection rates were similar, we observed opacification of all aneurysmal walls on 40% of the projection images in the 8-second rotation and in 51% of the projection images in the 14-second rotation.

The number of projection images acquired during a rotational run defines the geometric precision of the 3D reconstruction. This influence is based on the sampling theorem known from CT imaging (15).

The injection protocols were designed to be applicable in clinical examinations. A study of patient

tolerance of the prolonged injection of contrast material during RA has revealed no adverse reactions and no changes in blood pressure, intracranial pressure, or laboratory data after the injection of 3–5 mL/s over 6 seconds (16). Today, the reported injection parameters applied in clinical studies vary between 3 mL/s over 5 seconds (2, 4) and 4–5 mL/s over 8 seconds (3); most patients are under general anesthesia. In our clinical experience, alert patients experience discomfort and transient visual disturbances with higher amounts of contrast material; therefore, we perform 5- or 8-second rotations with 20 mL in alert patients and 14-second rotations with 35 mL only in patients under general anesthesia.

The key to the accurate 3D depiction of an aneurysm is to maximize filling of the aneurysmal sac with contrast material during the entire rotational cycle. The injection technique with an initial bolus improved visualization of the aneurysms on the 3D reconstructions, compared with continuous-flow technique. The reason for this effect could be observed on the projection images, which showed that the bolus injection resulted in earlier filling of the aneurysm with contrast material relative to initiation of image acquisition. The impact of the bolus technique was most noticeable in the 5- and 8-second runs. In the 14-second rotation, a longer rotational run and a higher number of projection images seemed to outweigh the influence of the injection technique.

The velocity with which the bolus is delivered also influences image quality. In the standard protocols, we selected bolus velocities beyond the systolic peak flow in the ICA of 7.9 mL/s. An additional experiment with a higher bolus velocity of 10 mL/s in the 8-second run resulted in 3D reconstructions with a blurred appearance. This may have been due to the disruption of flow in the ICA.

The results of the additional studies of the lateral aneurysm with a narrow neck underline the importance of early aneurysm filling. Improved visualization with more solid filling of the distal third of the aneurysmal lumen was achieved after the injection of an extra bolus of 5 mL/s over 2 seconds before the start of acquisition. These observations indicate that the timing of contrast material arrival in relation to start of image acquisition is likely to be a key variable for future study.

The models allowed the evaluation of the A2 and M2 branches. These branch vessels could be adequately visualized in the 5-second rotation (Fig 2A), with good agreement between the 3D measurements and the known values. More homogeneous contrast in the branch vessels and easier distinction from the background noise were achieved in the 8-second rotations (Fig 2B and C). The 14-seconds rotation provided no additional information concerning the anatomy of the branch vessels.

The results concerning the visualization of various types of saccular aneurysms with 3D RA confirm that the intra-aneurysmal hemodynamics depend on the geometric relationship between the aneurysm and the parent artery (7). We found distinct patterns of visualization in the bifurcation and lateral aneurysms, as well as a correlation between aneurysmal filling and the width of the ostium in both groups.

These findings are comparable to those of angiographic and duplex studies of flow patterns and velocities in silicone and canine aneurysm models (9, 17, 18) and in computer simulations (19, 20). In bifurcation and terminal aneurysms, Strother et al (9) describe a rapid intra-aneurysmal circulation without vortex formation or stasis. Although no distinct inflow or outflow pattern could be observed angiographically, Doppler studies revealed inflow at the edge of the ostium closest to the long axis of the parent artery, rotatory flow in the lumen, and outflow through the opposite corner.

In both aneurysm models of the MCA bifurcation, filling of the aneurysm with contrast material was too fast on the projection images to allow the delineation of a flow pattern. On the 3D reconstructions, we saw filling defects distant to the inflow zone; these were less prominent in the large-necked model because of the higher volume of flow through the larger ostium. These hemodynamically induced visualization deficits could be overcome by using the bolus-injection technique, and complete depiction of the aneurysm was achieved with the 5-second rotation in the large-necked model and with the 8-second rotation in the small-necked model.

In lateral aneurysms Strother et al (9) describe a regular flow pattern with inflow at the distal extent of the ostium, slow vortical flow in the center, and outflow along the aneurysm walls. Computer modeling of flow fields in lateral aneurysms with ostia of different sizes confirmed these results and demonstrated higher volumes of flow into the aneurysm with ostia of increased width (10). The restriction in this computer model was the assumption of a steady-flow state.

In the giant lateral aneurysm with a small neck, filling on the projection images followed this pattern, with a stagnating flow between the distal wall and the center of the aneurysm. Consequently, only the distal aneurysmal shell could be accurately depicted on the 3D reconstructions. The contrast attenuation along the proximal wall (which could be visualized with wider rendering windows) was too low to achieve a correct reconstruction, and it would not allow its differentiation from background noise in a clinical study.

This hemodynamic pattern proved to be the determinant in all rotational studies, and neither the application of high volumes of contrast material (5 mL/s in the eight and 14 seconds rotations) nor the injection of a bolus before the start of acquisition could provide a complete 3D depiction of the shape of the aneurysm.

Aneurysms of similar shape are found mostly in the cavernous and supraclinoid segments of the ICA. Those parts of the lumen distant to the inflow zone that may remain undetected by RA are prone to thrombus formation; therefore, they can escape visualization on endoluminal contrast images. In a study

of the correlation between 3D RA results and intra-operative findings, Tanoue et al (11) reported one case in which a discrepant finding regarding the shape of the aneurysm was due to an intraluminal thrombus. Thrombus formation may trigger wall thickening and aneurysmal growth (21). The frequent occurrence of large and giant aneurysms in the ICA may be explained by the fact that this site favors geometric conditions between the parent artery and the aneurysm that induce vortical, stagnating flow (9).

The flow pattern in the wide-necked lateral aneurysm with rapid filling on the projection images and complete depiction of its shape on the 3D reconstruction is due to high volume flow through the large ostium (10, 17). The lobulated aneurysm with a medium-sized ostium of the large sac and a wide ostium of the lobule combines both flow patterns, with only partial depiction of the large sac and more homogeneous filling of the lobule.

Considering clinical diagnostic procedures and the results of this study, we recommend the use of bolus technique for the injection of contrast material for RA. This technique improves filling of vessels and aneurysms, and it allows us to achieve high-resolution 3D reconstructions with the use of 20 mL of contrast agent for 5- and 8-second sweeps. This application seems to be of particular interest for the examination of alert patients who might not tolerate the larger amount of contrast material needed for the 14-second runs. The geometric relationship between the parent artery and the aneurysm, however, is the decisive factor that influences the representation of aneurysm with 3D RA. Whereas aneurysms with a bifurcation geometry (such as those found in most lesions in the MCA and ACA territories) can be depicted with high accuracy, the visualization of lateral aneurysms with a small neck may be incomplete, even after application of the bolus technique and long rotational runs. This possible restriction should be considered when 3D measurements are obtained for treatment planning. This is also of interest in the application of volumetric techniques, which depend on the homogeneity of contrast in the voxels of the reconstruction volume.

Conclusion

The injection of contrast material with an initial-bolus technique improves the depiction of aneurysms, in comparison with the continuous-flow technique. The geometric relationship between the aneurysm and the parent artery, which determines the hemodynamic pattern, is decisive in the visualization of aneurysms with 3D RA. Bifurcation aneurysms can be reliably depicted by using 20 mL of contrast agent. In lateral aneurysms, the anatomic accuracy of 3D visualization depends on the width of the ostium. In large aneurysms with a small neck, reconstructions may be incomplete, even after the application of high flow rates of contrast material.

References

1. Hoff DJ, Wallace C, ter Brugge K, Gentili F. **Rotational angiography assessment of cerebral aneurysms.** *AJNR Am J Neuroradiol* 1994;15:1945–1948
2. Anxionnat R, Bracard S, Macho J, et al. **3D Angiography. Clinical interest. First application in interventional neuroradiology.** *J Neuroradiol* 1998;25:251–262
3. Ishihara S, Ross JB, Piotin M, Weill A, Aerts H, Moret J. **3D Rotational angiography: recent experience in the evaluation of cerebral aneurysms for treatment.** *Intervent Neuroradiol* 2000;6: 85–94
4. Anxionnat R, Bracard S, Ducrocq X, et al. **Intracranial aneurysms: clinical value of 3D digital subtraction angiography in the therapeutic decision and endovascular treatment.** *Radiology* 2001;218: 799–808
5. Fahrig R, Fox AJ, Lownie S, Holdsworth DW. **Use of a C-arm system to generate true three-dimensional computed rotational angiograms: preliminary in vitro and in vivo results.** *AJNR Am J Neuroradiol* 1997;18:1507–1514
6. Bidault LM, Laurent C, Piotin M, et al. **Second-generation three-dimensional reconstruction for rotational three-dimensional angiography.** *Acad Radiol* 1998;5:836–849
7. Steiger HJ, Reulen HJ. **Low frequency flow fluctuation in saccular aneurysms.** *Acta Neurochir* 1986;83:131–137
8. Liepsch DW, Steiger HJ, Poll A, Reulen HJ. **Hemodynamic stress in lateral saccular aneurysms.** *Biorheology* 1987;24:689–710
9. Strother CM, Graves VB, Rappe A. **Aneurysm hemodynamics: an experimental study.** *AJNR Am J Neuroradiol* 1992;13:1089–1095
10. Burleson AC, Strother CM, Turitto VT. **Computer modeling of intracranial saccular and lateral aneurysms for the study of their hemodynamics.** *Neurosurgery* 1995;37:774–784
11. Tanoue S, Kiyosue H, Kenai H, Nakamura T, Yamashita M, Mori H. **Three-dimensional reconstructed images after rotational angiography in the evaluation of intracranial aneurysms: surgical correlation.** *Neurosurgery* 2000;47:866–871
12. Gailloud P, Pray JR, Muster M, Piotin M, Fasel JHD, Rüfenacht DA. **An in vitro anatomic model of the human cerebral arteries with saccular arterial aneurysms.** *Surg Radiol Anat* 1997;19:119–121
13. Holdsworth DW, Rickey DW, Drangova M, Miller DJM, Fenster A. **Computer-controlled positive displacement pump for physiological flow simulation.** *Med Biol Eng Comput* 1991;29:565–575
14. Ku DN, Giddens DP, Zarins CK, Glagov S. **Pulsatile flow and atherosclerosis in the human carotid bifurcation: positive correlation between plaque location and low and oscillating shear stress.** *Arteriosclerosis* 1985;5:293–302
15. Rosenfeld A, Kak AC. Digital Picture Processing. New York: Academic Press; 1976
16. Tu RK, Cohen WA, Maravilla KR, et al. **Digital subtraction rotational angiography for aneurysms of the intracranial anterior circulation: injection method and optimization.** *AJNR Am J Neuroradiol* 1996;17:1127–1136
17. Hashimoto T. **Dynamic measurement of pressure and flow velocities in glass and silastic model berry aneurysms.** *Neurol Res* 1984; 6:22–28
18. Graves VB, Strother CM, Partington CR, Rappe A. **Flow dynamics of lateral carotid artery aneurysms and their effects on coils and balloons: an experimental study in dogs.** *AJNR Am J Neuroradiol* 1992;13:189–196
19. Perktold K, Gruber K, Kenner T, Florian H. **Calculation of pulsatile flow and particle paths in an aneurysm model.** *Basic Res Cardiol* 1984;79:253–261
20. Gonzalez CF, Cho YI, Ortega HV, Moret J. **Intracranial aneurysms: flow analysis of their origin and progression.** *AJNR Am J Neuroradiol* 1992;13:181–188
21. Artmann H, Vonofakos D, Muller H, Grau H. **Neuroradiologic and neuropathological findings with growing giant intracranial aneurysm: review of the literature.** *Surg Neurol* 1984;21:391–401